

## A 7.8 kV nanosecond pulse generator with a 500 Hz repetition rate

To cite this article: M. Lin *et al*/2018 *JINST* **13** P04004

View the [article online](#) for updates and enhancements.

### Related content

- [Development of a 400 kV 80 mA Cockcroft-Walton power supply and 12 kW isolation transformer systems for neutron generators](#)  
X. Lu, S. Chen, Y. Zhang *et al.*
- [Design development and testing of high voltage power supply with crowbar protection for IOT based RF amplifier system in VECC](#)  
S.K. Thakur and Y. Kumar
- [The design and operation of a compact high-voltage, high pulse repetition frequency trigger generator](#)  
S J MacGregor, J M Koutsoubis and S M Turnbull



**IOP | ebooks™**

Bringing you innovative digital publishing with leading voices to create your essential collection of books in STEM research.

Start exploring the collection - download the first chapter of every title for free.

## A 7.8 kV nanosecond pulse generator with a 500 Hz repetition rate

M. Lin,<sup>a</sup> H. Liao,<sup>a</sup> M. Liu,<sup>a</sup> G. Zhu,<sup>a</sup> Z. Yang,<sup>a</sup> P. Shi,<sup>a</sup> Q. Lu,<sup>b</sup> and X. Sun<sup>a,b,1</sup>

<sup>a</sup>Department of Modern Physics, University of Science and Technology of China, Hefei 230026, China

<sup>b</sup>CAS Key Laboratory of Geospace Environment, No. 96, JinZhai Road Baohe District, Hefei 230026, China

E-mail: [xsun@ustc.edu.cn](mailto:xsun@ustc.edu.cn)

**ABSTRACT:** Pseudospark switches are widely used in pulsed power applications. In this paper, we present the design and performance of a 500 Hz repetition rate high-voltage pulse generator to drive TDI-series pseudospark switches. A high-voltage pulse is produced by discharging an 8  $\mu\text{F}$  capacitor through a primary windings of a setup isolation transformer using a single metal-oxide-semiconductor field-effect transistor (MOSFET) as a control switch. In addition, a self-break spark gap is used to steepen the pulse front. The pulse generator can deliver a high-voltage pulse with a peak trigger voltage of 7.8 kV, a peak trigger current of 63 A, a full width at half maximum (FWHM) of  $\sim 30$  ns, and a rise time of 5 ns to the trigger pin of the pseudospark switch. During burst mode operation, the generator achieved up to a 500 Hz repetition rate. Meanwhile, we also provide an AC heater power circuit for heating a  $\text{H}_2$  reservoir. This pulse generator can be used in circuits with TDI-series pseudospark switches with either a grounded cathode or with a cathode electrically floating operation. The details of the circuits and their implementation are described in the paper.

**KEYWORDS:** Pulsed power; Trigger concepts and systems (hardware and software); Plasma generation (laser-produced, RF, x ray-produced)

<sup>1</sup>Corresponding author.

---

## Contents

<b>1</b>	<b>Introduction</b>	<b>1</b>
<b>2</b>	<b>Pulse generator circuit and analysis</b>	<b>2</b>
<b>3</b>	<b>Experimental arrangement and results</b>	<b>3</b>
3.1	Single-shot operation	3
3.2	Jitter	6
3.3	Repetition-rate operation	7
<b>4</b>	<b>Conclusion</b>	<b>9</b>

---

## 1 Introduction

High-voltage and high-current switches are the key components of pulsed power technology applications. However, there are only very few types of switches that can be used in such a field. TDI-series pseudospark switches [1, 2], also known as cold cathode thyratrons, provide a unique high current (up to 200 kA) with a high charge transfer capability (more than  $10^6\text{C}$ ) with superior time stability (time jitter  $< 3$  ns) and are used as a switch tube in the pulse circuits of capacitive storages with submicrosecond and microsecond pulse durations with an anode voltage in the range of 3 to 150 kV. A pseudospark switch provides a wide number of perspective applications in pulsed power applications, including high-power pulsed lasers, plasma focus, shock wave generators, and high-intensity electron beams for materials processing and crowbar protection, and has attracted increasing attention. TDI-series pseudospark switches are commercially available at low cost with small overall dimensions and to a certain extent, can replace ignitions and triggered spark gaps, vacuum and pressurized switches, etc. Triggering a pseudospark requires a trigger voltage with a negative polarity. The trigger voltage must not be less than 4 kV, and the current must not be less than 50 A. If  $dV/dt$  is greater than  $5\text{ kV}/\mu\text{s}$  [3], then a high-voltage pulse generator that maintains a steady and reliable performance is meaningful and crucial.

Several techniques have been used to switch high-current switches. J. Chatzakis et al. [4] reported that ten SGW30N60 IGBTs (insulated gate bipolar transistors) connected in parallel with a self-break spark gap to sharpen the pulses coming from the isolation transformer were used to trigger the pseudospark (TDI1-150k/25). The main specifications of the pulse amplitude, rise time, pulse width and jitter are 5 kV, 10 ns, 300 ns, and  $\sim 50$  ns into a  $100\ \Omega$  load, respectively. Vernon H. Chaplin et al. [5] demonstrated that a circuit that uses two IXYS IXEL40N400 IGBTs connected in parallel delivered a 230 A peak to the ignitron trigger with rise time of  $\sim 0.6\ \mu\text{s}$ . A silicon-controlled rectifier (SCR) was also used to trigger a pseudospark in a KMAX-FRC pulsed power system [6] with an 8 kV trigger voltage and 85 A current with a current rise time of  $\sim 2\ \mu\text{s}$  [7]. Other high-voltage pulse forming techniques have also been mentioned [8–14].

In this paper, we present a new design approach that uses a single MOSFET combined with a self-break spark gap achieving a high-voltage pulse with a rise time of 5 ns, a full width at half maximum (FWHM) of  $\sim 30$  ns, a peak trigger voltage of 7.8 kV, and a peak trigger current of 63 A to trigger a pseudospark. The use of a single MOSFET contributes to miniaturization of the equipment and smaller power dissipation. Moreover, the single MOSFET helps simplify the equipment with a compact design at a low cost. In addition, the high-voltage pulse generator can be operated either by a built-in generator or by an external 1 mm plastic fiber optic signal via HFBR-25X1ETZ receiver. The remaining three sections of the paper are organized as follows. The pulse generator circuit and analysis will be presented in section 2, and the experimental arrangement and results are presented in section 3. Finally, a summary is presented in section 4.

## 2 Pulse generator circuit and analysis

The power MOSFET (IXYS IXFX80N60P3) rated for 600 V with an average current rating of 80 A, and a peak current of 200 A has been selected for the pulse generator switch. In this pulse generator, the actual operating voltage is approximately 330 V, which ensures a safe margin of the operation for the MOSFET. Meanwhile, a type TX-DA962Dn MOSFET gate driver (Beijing LMY Electronics Co., LTD) is used to turn on the MOSFET. The pulse generator circuit diagram is shown in figure 1. For part (a), the 220 V alternating current (AC) rectified by a bridge rectifier D1 and filtered by an electrolytic capacitor (300  $\mu$ F/450 V) C2 will charge the 8  $\mu$ F capacitor C1 that provides the energy to trigger the pseudospark. The resistors R1 and R2 could be regarded as a charging resistance that limits the charging current of the capacitor C1. Moreover, the resistor R2 inserted in the discharging circuit simultaneously can dampen the oscillation of the circuit and achieve a faster recovery time. For the sake of a steepening the pulse front, a homemade self-break spark gap was used to steepen the pulses on the order of a microsecond coming from the pulse transformer. The spark gap is made up of two stainless steel spheres, and the distance between two electrodes is about 3 mm. Once MOSFET is switched on, the energy stored in capacitor C1 is transferred to the primary windings of the step-up transformer T1 (1:30, measuring with a 5 M $\Omega$  load resistor), and then the secondary windings will output a higher voltage signal, approximately several kilovolts. Once the voltage at both ends of the spark gap reaches a certain value, the spark gap will be self-breaking, and then the heated pseudospark will be fired. The capacitor C4 (220 pF/50 kV) connected in parallel to the secondary winding of the step-up transformer T1 serves to absorb return pulses, and the decoupling capacitors C5 and C6 (4.7 nF/50 kV) close to the pseudospark are used to isolate the trigger system from the DC charging circuit of the pulsed power system. Because of the fast switching feature of the MOSFETs at turn-off, the instantaneous rate in current over time ( $di/dt$ ) would have a very high value. Therefore, the drain-source voltage will rise due to the back EMF from parasitic inductance. Proper attention needs to be paid to protecting the MOSFET from destruction. Hence, a RCD snubber circuit (consisting of a diode, D2, a 3.7  $\Omega$  resistance R3, and a 0.47  $\mu$ F capacitor C3) is connected in parallel at drain-source of the MOSFET to ensure that the MOSFET is turned off gently. In addition, five transient voltage suppression diodes D3 (P6KE550CA) connected in parallel are applied in the circuit to react to sudden or momentary overvoltage conditions.

The reliability of the pulse generator to trigger the pseudospark is closely related to the heater current. A heater driver integrated inside the pulse generator is designed for heating a H<sub>2</sub> reservoir

that releases the working gas inside the pseudospark chamber. The electrical schematic of the heater driver is shown in figure 1(b). The order of the components from left to right are a voltage regulator T2, a 40 kV isolation transformer, T3, a 1 nF reservoir protection capacitor, C7, and a 525  $\mu$ H common mode choke coil L2. The output voltage ranges from 0–12 V, and the current ranges from 0–3 A. In addition, the heater voltage can be adjusted in steps of 0.05–0.1 V. The distinguishing factor with the previous heater driver [7] is that we added a common mode choke coil to suppress common mode noise. Therefore, the heater driver will supply a steadier heat current.

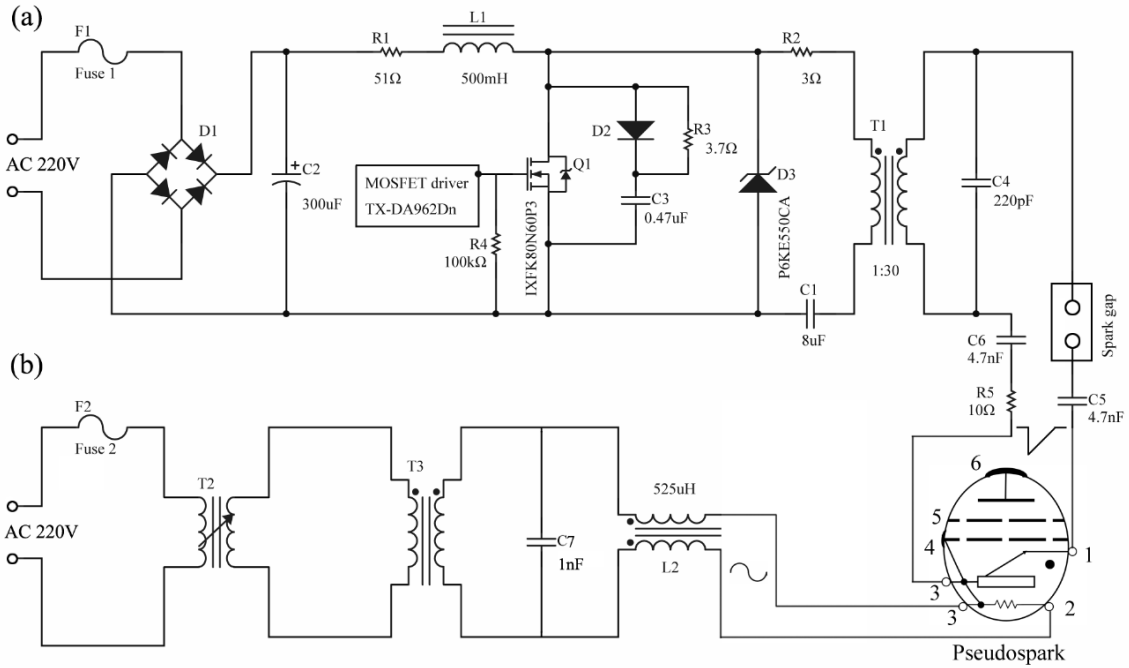


**Figure 1.** Circuit diagram of the pulse generator. Electrodes connection of the pseudospark: 1 - Igniter terminal for trigger negative pulse; 2 - Heater ( $R \sim 1\Omega$ ); 3 - Cathode pins; 4 - Cathode, heater, igniter terminal (+); 5 - Gradient grid; 6 - Anode.

### 3 Experimental arrangement and results

In this section, the performance of the pulse generator will be presented. Two kinds of high voltage probes, a HVP-15HF high-voltage probe (50 MHz bandwidth) or a Tektronix high-voltage probe (model P6015A, 75 MHz bandwidth), were used for voltage measurements, and a Pearson current monitor (model 4997, 1:100) was used for current measurements. All the measured signals are connected to a digital oscilloscope, Rigol DS4014 (100 MHz bandwidth and 4 GSa/s sample rate).

#### 3.1 Single-shot operation

In single-shot operation mode, a digital pulse generator outputs a single pulse signal with amplitude and width of 5 V and 50  $\mu$ s, respectively. Figure 2 shows the initial trigger signal (the black solid line) and the primary windings current (the blue solid line) of the step-up transformer T1 with a 200  $\Omega$  resistive dummy load. The rise time of the primary windings current is approximately 6  $\mu$ s,

and the peak current is approximately 100 A. Once the trigger signal ends, the current decreases immediately, indicating that the MOSFET circuit works properly. The dashed line in figure 2 indicates the moment of breakdown time of the self-break spark gap, corresponding to the time that the trigger output voltage starts to rise (see figure 4).

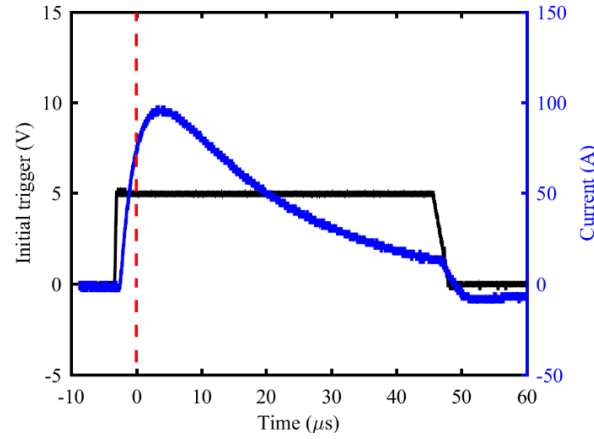


**Figure 2.** (Color online) The initial trigger voltage, shown as the black line, is the 5 V signal from the SRS DG645 pulse generator. The current is  $\sim 100$  A measured by a 1:100 Pearson current monitor. The dashed line indicates the moment of breakdown time of the self-break spark gap with a  $200\ \Omega$  resistive dummy load.

To find how the spark gap affects the rise time of the output trigger, we removed the spark gap, and connected the secondary windings of the step-up transformer and decoupling capacitors directly to the  $200\ \Omega$  load. As shown in figure 3, the trigger generator can deliver a pulse with a peak voltage of 1.6 kV, a peak current of 7.9 A, and a rise time of  $6\ \mu\text{s}$  to this load. The overall circuit efficiency can be defined as  $\eta = \frac{W}{\frac{1}{2}CU^2}$ , where  $W = \int U_{\text{tr}}I_{\text{tr}}dt \approx 0.20\text{J}$  ( $U_{\text{tr}}$  and  $I_{\text{tr}}$  are trigger voltage and current respectively), is the energy output by the step-up transformer; and  $\frac{1}{2}CU^2$  is the energy stored in the  $8\ \mu\text{F}$  capacitor C1, which is  $\sim 0.44\text{J}$ . Thus, the efficiency is  $\sim 45.5\%$ .

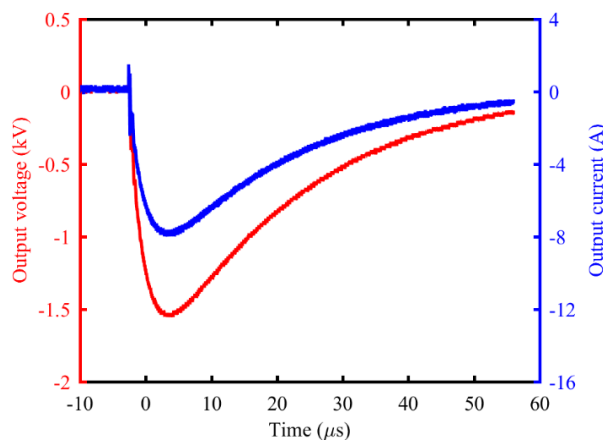


**Figure 3.** (Color online) Trigger voltage and current waveforms of the  $200\ \Omega$  resistive dummy load without the self-break spark gap. The amplitude and width of initial trigger are set to 5 V and  $100\ \mu\text{s}$ , respectively.

For the rest of the experiments the self-break spark gap was connected in the secondary windings of the step-up transformer. Figure 4 shows the voltage (red line) and the secondary windings current (blue line) of the load (also  $200\ \Omega$ ). The inset figure shows that the voltage has a steep rise time of approximately 5 ns. The output peak value can reach approximately 17.8 kV subsequently with a few oscillations and then return back to near zero. The rise time of the pulse front is mainly limited by the inductance of the self-break spark gap and connection cables. Compared to the case without spark gap, see figure 3, the rise time is reduced by three orders of magnitude. In other words, the self-break spark gap has a good steepening effect on the trigger pulse front.

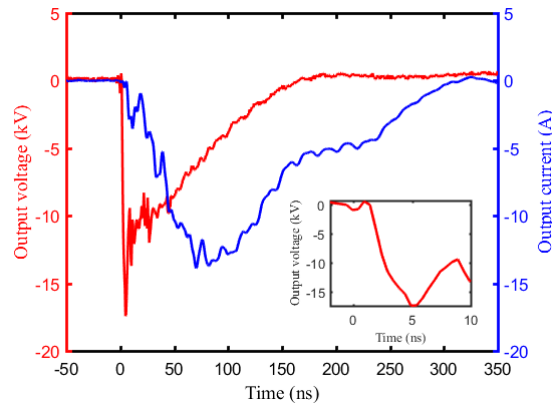


**Figure 4.** (Color online) Trigger voltage and current waveforms of the  $200\ \Omega$  resistive dummy load measured by the Tektronix high-voltage probe and the Pearson current monitor.

Next, the  $200\ \Omega$  load was replaced by the pseudospark (TDI4-100k/45H), and the entire circuit connection was just as the description in figure 1. The pseudospark was triggered after the heater was turned on and the pseudospark warmed up in approximately 5 minutes. Figure 5 shows the voltage (red line) and the secondary windings current (blue line) at pseudospark's igniter. In contrast to the signal in figure 4, the voltage signal at approximately 7.8 kV is much smaller, but the current signal is much larger.

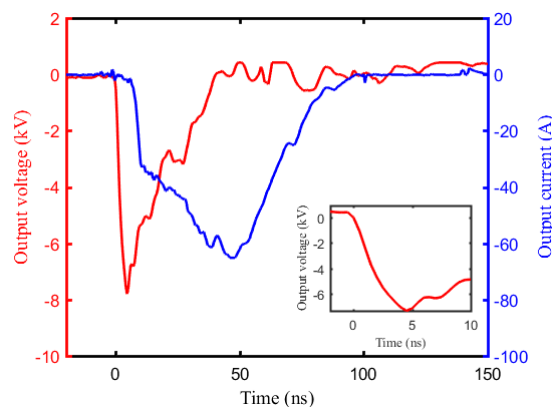


**Figure 5.** (Color online) Trigger voltage and current waveforms at the pseudospark's igniter, measured by the Tektronix high-voltage probe and the Pearson current monitor.

To further demonstrate the performance of the pulse generator, the pseudospark was used to trigger a charged capacitor to discharge, so it is connected with a  $5\ \mu\text{F}$  high-voltage power capacitor and a  $2\ \mu\text{H}$  air core inductor in series. Figure 6 shows the measured discharging currents with six different voltages of the  $5\ \mu\text{F}$  capacitor. We see that capacitor starts to discharge almost at the same time in every shot with an increase in the voltage, which has proved our pulse generator can successfully trigger a pseudospark to help the high-voltage power capacitor discharge accurately.

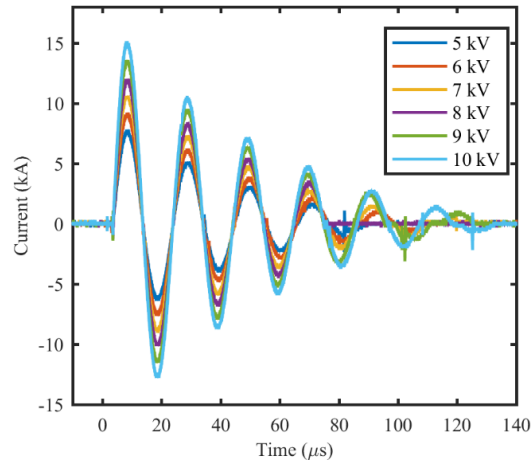


**Figure 6.** (Color online) Measured discharging currents of the high-voltage power capacitor ( $5\ \mu\text{F}$ ). The load is a  $2\ \mu\text{H}$  air core inductor.

### 3.2 Jitter

Jitter, which can be quantified by peak-to-peak time displacement, is an important factor in the design of high voltage pulse generator. To find the jitter of this pulse generator, we have performed 35 shots continuously in single-shot operation mode. The data points in figure 7 represent the time variation of the 35 consecutive trigger voltage start-ups. Clearly, the jitter is less than 50 ns. If the

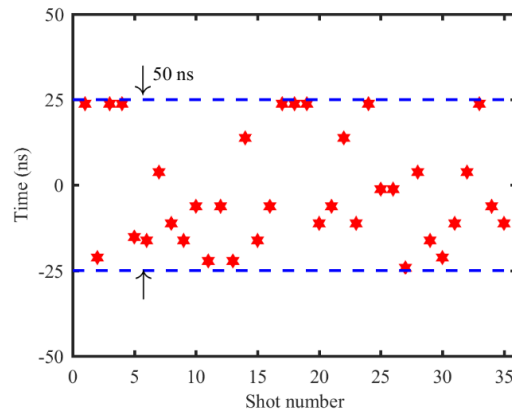


**Figure 7.** (Color online) Jitter of the pulse generator, which is approximately 50 ns.



self-break spark gap is removed from the circuit, then the jitter became less than 1 ns. In other words, most of the jitter of the pulse generator circuit comes from the self-break spark gap itself. Thus, if a lower jitter is needed for a special purpose, the circuit can be upgraded by optimizing the homemade spark gap or substituting with another spark gap with a lower jitter.

### 3.3 Repetition-rate operation

The repetition-rate test was performed with a  $200\ \Omega$  load, and the experimental results of the 500 Hz operation are shown in figure 8. The voltage signal plot is on top, and the current signal plot is on the bottom with multiple pulses in one shot. In this figure, only 8 waveforms are presented, which are not identical but are relatively steady. This finding can be understood since the voltage on the  $8\ \mu\text{F}$  capacitor is changed after each discharge. For 1 kHz repetition-rate operation, as shown in figure 9, the situation becomes slightly more severe, and sometimes the generator could fail to deliver a pulse. We also used NI Multisim to perform a circuit simulation with a circuit similar to that in figure 1, but the replacement of the load with a  $200\ \Omega$  resistor and the spark gap were removed. The results are shown in figure 10. During operation at 500 Hz, the simulation result (the red one) is consistent with the results of the experiment. During operation at 1 kHz, the simulation result (the blue one) and the experiment result are both insufficient.

The main characteristics of the high-voltage pulse generator are summarized in table 1.

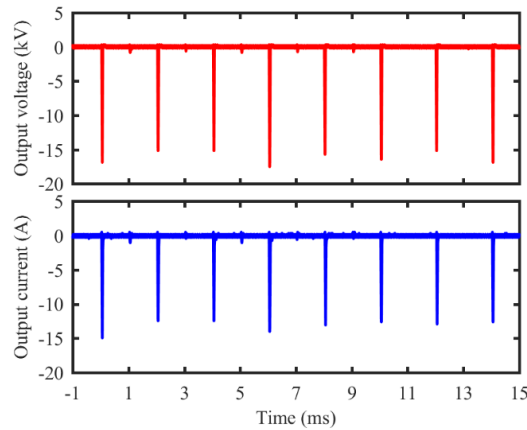


**Figure 8.** (Color online) Repetition-rate test at 500 Hz operation. Output voltage and current of the  $200\ \Omega$  resistive dummy load, measured by the HVP-15HF high-voltage probe and the Pearson current monitor.

The repetition-rate of this pulse generator is mainly limited by two factors: the charging time  $t_c$  of the  $8\ \mu\text{F}$  capacitor and the recovery time  $t_r$  of the spark gap. The capacitor should be fully charged before the MOSFET is switched on. The voltage on the capacitor is  $U_c = U_{\text{DC}} (1 - e^{-t_c/\tau})$ , where  $U_{\text{DC}}$  is the voltage of the power supply and  $\tau = RC$  is the time constant. The charging time  $t_c$  is usually  $(3 \sim 5)\tau$  or larger. For repetition rate of  $f = 500\ \text{Hz}$ , the available charging time is  $1/f = 2\ \text{ms}$ , then a minimum  $\tau$  of  $(\frac{1}{5f} \sim \frac{1}{3f}) = 0.4 \sim 0.67\ \text{ms}$  is required. In our trigger circuit, the  $\tau$  is  $0.43\ \text{ms}$ , suitable for the operation of  $f = 500\ \text{Hz}$ . If  $f = 1\ \text{kHz}$  is preferred, then the  $\tau$  should be  $< 0.2 \sim 0.33\ \text{ms}$ .

The recovery time of spark gap,  $t_r$ , is mainly determined by the cooling time of the hot channel formed by the spark. For gases such as air, nitrogen, and argon, typical recovery time are on the

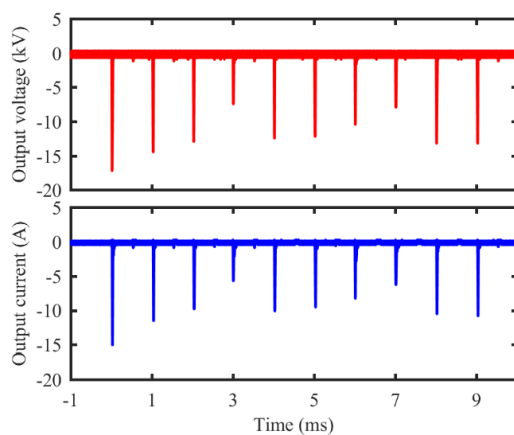


**Figure 9.** (Color online) Repetition-rate test at 1 kHz operation. Output voltage and current of the  $200\ \Omega$  resistive dummy load, measured by the HVP-15HF high-voltage probe and the Pearson current monitor.

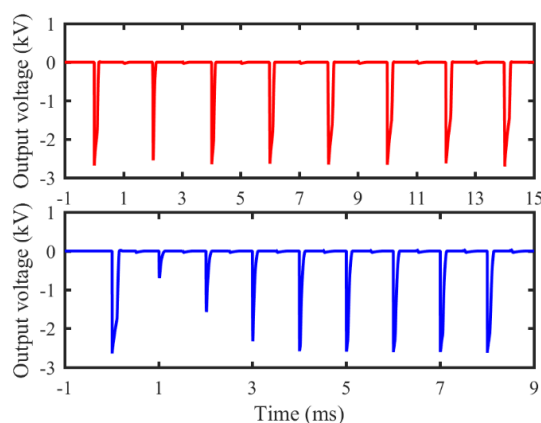


**Figure 10.** (Color online) Simulation results of 500 Hz and 1 kHz operations. Output voltage of the  $200\ \Omega$  resistive dummy load (without spark gap).

**Table 1.** Specifications of the pulse generator.

Parameter	Pseudospark operation
Peak trigger voltage	7.8 kV
Peak trigger current	63 A
FWHM	$\sim 30$ ns
Rise time	5 ns
Jitter	$\sim 50$ ns
Repetition-rate (typical)	500 Hz (with $200\ \Omega$ Resister)
Heater voltage	0–12 V
Heater current	0–3 A
Trigger mode	Optical/Electrical
Isolation	40 kV

order of 10 ms as reported by S. Moran et al. [15]. Various methods can be employed to reduce the recovery time, such as sweeping out the residual charges in the inter-pulse period [16], undervolting the switch [17], etc. Our self-break spark gap relies on the flow of open air to improve the recovery, though it has not been purposely optimized.

## 4 Conclusion

In summary, a high-voltage pulse generator using a single MOSFET combined with a self-break spark gap to trigger a pseudospark successfully is reported for the first time. The use of a single MOSFET contributes to miniaturization of the equipment and smaller power dissipation. Moreover, the single MOSFET helps simplify the equipment with a compact design at a low cost. The pulse generator combines a trigger circuit and an AC heater power circuit resulting in a fully integrated pseudospark generator package. The peak trigger voltage, peak trigger current, rise time, FWHM, jitter, and typical repetition-rate are 7.8 kV, 63 A, 5 ns,  $\sim 30$  ns, 50 ns, and 500 Hz, respectively. A jitter value of approximately 50 ns mainly comes from the homemade spark gap, and the repetition-rate is mainly limited by the charging time of the 8  $\mu$ F capacitor and recovery time of the self-break spark gap.

## Acknowledgments

This work is supported by the following: the Key Research Program of Frontier Sciences, CAS (QYZDJ-SSW-DQC010; the National Natural Science Foundation of China (NSFC) under Grant No. 11475172 and 41331067, and the National Key R&D Program of China under Contract No. 2017YFA0402500.

## References

- [1] V.D. Bochkov, Y.D. Korolev, K. Frank, O.B. Frants and I.A. Shemyakin, *Pseudospark switches for the power supply circuits of pulsed lasers*, *Russ. Phys. J.* **43** (2000) 432.
- [2] V.D. Bochkov, V. Dyagilev, V. Ushich, O. Frants, Y. Korolev, I. Sheirlyakin et al., et al., *Sealed-Off Pseudospark Switches for Pulsed Power Applications Current Status and Prospects*, *IEEE Trans. Plasma Sci.* **29** (2001) 802.
- [3] V.D. Bochkov et al., *Research and Development of Pseudospark Switch Drivers*, in *Proceedings of the 2012 IEEE International Power Modulator and High Voltage Conference*, San Diego, CA, U.S.A., 2012, pp. 552–554.
- [4] J. Chatzakis, S.M. Hassan, E.L. Clark, C. Petridis, P. Lee and M. Tatarakis, *High repetition rate pseudospark trigger generator*, *Rev. Sci. Instrum.* **79** (2008) 086103.
- [5] V.H. Chaplin and P.M. Bellan, *Fast ignitron trigger circuit using insulated gate bipolar transistors*, *IEEE Trans. Plasma Sci.* **41** (2013) 975.
- [6] M. Lin, M. Liu, G. Zhu, P. Shi, J. Zheng, Q. Lu et al., *Field-reversed configuration formed by in-vessel  $\theta$ -pinch in a tandem mirror device*, *Rev. Sci. Instrum.* **88** (2017) 093505.
- [7] M. Lin, M. Liu, G. Zhu, Y. Wang, P. Shi and X. Sun, *A high voltage pulse generator based on silicon-controlled rectifier for field-reversed configuration experiment*, *Rev. Sci. Instrum.* **88** (2017) 083507.

- [8] D.H. Barnett, J.M. Parson, C.F. Lynn, P.M. Kelly, M. Taylor, S. Calico et al., *Optically isolated, 2 kHz repetition rate, 4 kV solid-state pulse trigger generator*, *Rev. Sci. Instrum.* **86** (2015) 034702.
- [9] I. Boscolo and S. La Torre, *A 6 kV–150 A, 8 ns rise time pulse generator for excitation of ferroelectric cathodes*, *Rev. Sci. Instrum.* **70** (1999) 1857.
- [10] A. de Angelis, J.F. Kolb, L. Zeni and K.H. Schoenbach, *Kilovolt Blumlein pulse generator with variable pulse duration and polarity*, *Rev. Sci. Instrum.* **79** (2008) 044301.
- [11] R. Hironaka, M. Watanabe, A. Okino, M. Maeyama, K.-C. Ko and E. Hotta, *Performance of pulsed power generator using high voltage static induction thyristor*, *IEEE Trans. Plasma Sci.* **28** (2000) 1524.
- [12] J. Mao, X. Wang, D. Tang, H. Lv, C. Li, Y. Shao et al., *A compact, low jitter, nanosecond rise time, high voltage pulse generator with variable amplitude*, *Rev. Sci. Instrum.* **83** (2012) 075112.
- [13] D. Zhang, Y. Zhou, P. Yan, T. Shao, Y. Sun, Y. Zhou et al., *A compact, high repetition-rate, nanosecond pulse generator based on magnetic pulse compression*, *IEEE Trans. Plasma Sci.* **45** (2017) 1601.
- [14] Y. Zhang, J. Liu, X. Cheng, G. Bai, H. Zhang, J. Feng et al., *A compact high-voltage pulse generator based on pulse transformer with closed magnetic core*, *Rev. Sci. Instrum.* **81** (2010) 033302.
- [15] S.L. Moran, L.W. Hardesty and M.G. Grothaus, *Hydrogen Spark Gap for High Repetition Rates*, in *Proceedings of the 8<sup>th</sup> International IEEE Pulse Power Conference*, San Diego, CA, U.S.A., 1991, p. 336–339.
- [16] S.J. MacGregor, S.M. Tumbull, F.A. Tuema and O. Farish, *The Operation of Repetitive High Pressure Gas Switches*, *J. Phys.* **D 26** (1993) 954.
- [17] M.G. Grothaus, S.L. Moran, and L.W. Hardesty, *Recovery Characteristics of Hydrogen Spark Gap Switches*, in *Proceedings of the 9<sup>th</sup> International IEEE Pulse Power Conference*, Albuquerque, NM, U.S.A., 1993, pp. 475–478.